THE JOURNAL OF NAVIGATION (2007), **60**, 327–348. © The Royal Institute of Navigation
doi:10.1017/S0373463307004237 Printed in the United Kingdom

Failure Modes and Models for Integrated GPS/INS Systems

Umar Iqbal Bhatti and Washington Yotto Ochieng

(*Imperial College London*)
(Email: w.ochieng@imperial.ac.uk)

GPS is the most widely used global navigation satellite system. By design, there is no provision for real time integrity information within the Standard Positioning Service (SPS). However, in safety critical sectors like aviation, stringent integrity performance requirements must be met. This can be achieved externally or at the receiver level through receiver autonomous integrity monitoring (RAIM). The latter is a cost effective method that relies on data consistency, and therefore requires redundant measurements. An external aid to provide this redundancy can be in the form of an Inertial Navigation System (INS). This should enable continued performance even during RAIM holes (when no redundant satellite measurements are available). However, due to the inclusion of an additional system and the coupling mechanism, integrity issues become more challenging. To develop an effective integrity monitoring capability, a good understanding of the potential failure modes of the integrated system is vital. In this paper potential failure modes of integrated GPS/INS systems are identified. This is followed by the specification of corresponding models that would be required to investigate the capability of existing integrity algorithms and to develop enhancements or new algorithms.

KEY WORDS

1. GPS 2. Inertial navigation systems 3. Failure modes

1. INTRODUCTION. The Global Positioning System (GPS) today is the only fully operational satellite based navigation system. However, due to the recent shift in focus of worldwide aviation from ground based to space based navigation systems, the safety of use of GPS for such purposes has currently become the subject of global research. GPS performance available to the civilian community is specified in the SPS Performance Standard (US DoD, 2001) providing information on service accuracy, availability and reliability with respect to the signal-in-space (SIS).

To use GPS for aviation, stringent standards, established by the International Civil Aviation Organization (ICAO), have to be met (ICAO, SARPS, 2004). One of the requirements is integrity, a measure of the degree of trust that can be placed in the correctness of the navigation information. However, the GPS SPS does not provide real time integrity information. Hence, for safety critical applications like aviation, GPS signals must be monitored. The vulnerability of GPS signals has been investigated for example by Ochieng et al. (2003) and Volpe (2001). Furthermore, recent research has focussed on the quantification of the failure modes of GPS (Ochieng et al., 2003; Van Dyke et al., 2004). These studies are based on exhaustive search for potential failure modes that can significantly affect GPS navigation performance. In this regard work on Integrity Failure Modes and Effect Analysis (IFMEA) for the complex and multi-segmented GPS is still ongoing.

GPS augmentations like Ground Based Augmentation Systems (GBAS) and Satellite Based Augmentation Systems (SBAS) monitor GPS signals in real time. They relay integrity information using signals which are themselves vulnerable to jamming and interference, a principal failure mode of GPS. Hence a potentially effective method to address the exposure to such risks is to integrate GPS with other sensors such as INS.

The INS is a self contained system with high short term stability, immune to jamming as well as interference. However, high grade systems are very expensive. The emergence of INS sensors exploiting Micro-Electromechanical Systems (MEMS) technology is creating the potential for affordable integrated GPS/INS architectures if the problems associated with performance could be overcome. This has the potential to offer a cost effective alternative to other forms of augmentations depending on the user (operational) requirements.

INS can be integrated synergistically with GPS so that short term and long term stabilities of INS and GPS respectively, can be exploited. The traditional integration method is the usage of a Kalman filter. In order to realise an optimal integrated system, a number of issues need to be considered. These include the type of INS and the integration architecture, which have implications on system integrity. Various types of integration methods are available, broadly classified as loosely coupled, tightly coupled and ultra-tightly/deeply coupled. Loosely coupled systems combine processed measurements of the two systems while tightly coupled systems generally carry out the integration at the raw measurement level. Ultra-tight systems generally have feedback loops between the two systems.

The performance of the tightly coupled system has been shown to be better than that of the loosely coupled system as far as the availability of integrity information is concerned (Lee et al., 2004). The latter requires at least four GPS satellites to be available to provide a 3-dimensional position solution. On the other hand, tightly coupled systems can produce an integrated position determination with less than four satellites. Ultra-tight coupling in general, outperforms tightly coupled systems with regard to operation in noisy environments and their anti-jamming capabilities (Gustafson, et al., 2003). However, the integrity monitoring in this case becomes complicated because GPS observables are contaminated by inertial errors.

The threats to system integrity are failure modes. Such failures can emanate from the systems, operational environments and human factors. Note that for an integrated system, the analysis of failure modes should consider not only failures related to the systems separately but also to the integrated architecture. This paper presents a high level analysis of failure modes. The potential failure modes of individual systems are presented along with their description and potential impact. These include failure modes of GPS, INS (hardware and operational), the emerging class of INS based on MEMS technology and those that arise due to the coupling of the GPS and INS. The next logical step taken in this regard is the characterization of these failure modes. These are categorized and approximate mathematical formulae

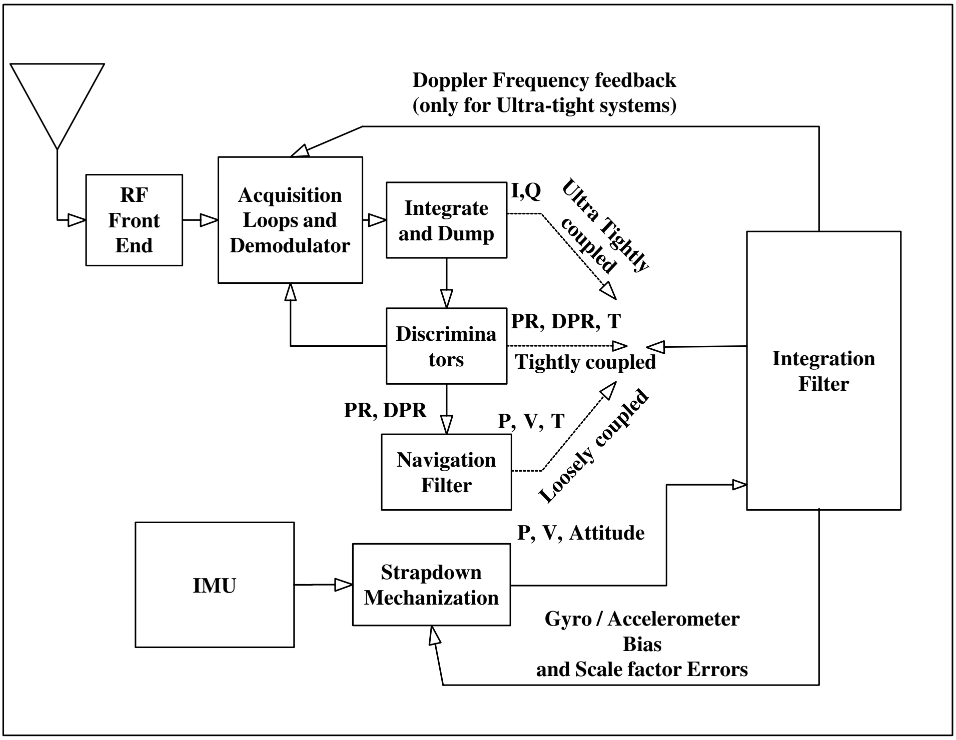

Figure 1. Loose, Tight and Ultra-Tight GPS/INS navigation system (Modified from Babu et al., 2004).

suggested for failure models that can be used to investigate the capability of integrity algorithms and to develop either enhancements or new algorithms.

The rest of the paper presents the various integration architectures, followed by the various failure modes of GPS, INS and the integrated system. The failure modes are then characterized in the form of mathematical models.

2. INTEGRATION ARCHITECTURES.

Traditionally GPS and INS are coupled through a Kalman filter to obtain position, velocity and time. Initially, two broad classes of integration, loose and tight coupling, were developed. However, in recent years, a third class has emerged, referred to as deep integration or ultra-tight integration.

Figure 1 shows the three configurations at a high level. In the figure, the radio frequency (RF) front end refers to the electronic circuitry in the GPS receiver that is used to down-covert the GPS signal carrier frequency to a lower frequency called Intermediate Frequency (IF). This is done in order to avoid expensive receivers that may be required to process the signal in the GPS carrier frequency range. The acquisition and demodulator block tracks the input signal by monitoring the error between the received signal and the replica signal generated internally by the receiver. The received signal is also multiplied (demodulated) with the said replica signal. The

https://doi.org/10.1017/S0373463307004237 Published online by Cambridge University Press

Integrate and Dump (I & D) filter averages the signal obtained from the demodulator to produce the average in-phase and quadrature phase components of the demodulated signal. This is to enable the discriminator algorithm to decode the time delay between the internally generated code signal and the code signal obtained from the received signal. The pseudorange (PR) and delta pseudorange (DPR) measurements obtained from the discriminator are then used by the navigation filter to produce position, velocity and time of the host vehicle. In parallel, velocity and attitude increments are obtained from the inertial measurement unit (IMU) to act as forcing function in the navigation differential equations to generate attitude, velocity and position. Also in the navigation processor, error compensation equations are used to refine IMU measurements. The integration filter is used to combine measurements from GPS and INS.

In Figure 1, the interconnections for different couplings are labelled to clarify the depth of integration. In the case of loosely coupled systems, the position, velocity and time from the GPS receiver are combined with position, velocity and attitude from INS by use of a truth model. The truth model is a mathematical depiction of the error characteristics of the systems that are to be combined by a Kalman filter. For a tightly coupled system, position, velocity and time from the INS are combined with the GPS pseudorange measurements by using a Kalman filter. In ultra-tight coupling, the measurements from the GPS receiver used are the in-phase, I, and quadrature-phase, Q, signals. There are variants of ultra-tight or deep integration. The salient difference between these couplings is the method of combining INS and GPS observables. In Gustafson et al. (2003) a minimum variance non-linear filter is used, while in Kim et al. (2003) an extended Kalman filter is employed. Gold et al. (2004) utilize cascaded Kalman filter stages.

2.1. *Loosely Coupled System.* In this configuration, the outputs of the two systems are combined in the navigation processor, typically a Kalman filter. In essence, the position solution from GPS and INS are subtracted to provide the error used to estimate the states of the integrated system to provide required navigation variables. A disadvantage of the loosely coupled system is that the Kalman filter heavily depends upon the GPS solution. Hence, if the GPS solution is not available (e.g. when less than four satellites are available) the integrated solution is no longer possible. In such a case the performance of the integrated system is limited to its coasting capability. The time for which a system can coast depends primarily on the quality of the inertial sensors. The loosely coupled system is based on position domain coupling, and provides benefits over individual systems. These benefits are in terms of navigation performance i.e. accuracy, integrity, continuity and availability. This means that the integrated system

- is more accurate,
- has a high integrity provided by an additional navigation system,
- is capable of a higher rate than GPS because of the higher data rate of INS,
- should be available even during GPS outage for a period limited by the quality of the INS.

However, to get real benefits in integrity monitoring, measurement domain coupling methods are recommended.

2.2. *Tightly Coupled System.* In the tightly coupled system, raw GPS measurements (i.e. pseudoranges and pseudorange rates) are provided to the integration filter

https://doi.org/10.1017/S0373463307004237 Published online by Cambridge University Press

directly. The error states for the GPS receiver clock drift and bias are also included in addition to the states in the loosely coupled system. The Kalman filter processes GPS raw measurements and their corresponding values predicted from INS measurements. The latter is made possible by using the current position as determined by the INS and the ephemeris data. In this way, even with fewer than four available satellites, the navigation solution can be maintained by the Kalman filter. A disadvantage of this filter is that it responds more slowly to INS errors than the loosely coupled system (Gautier, 2003). However, with respect to integrity monitoring performance, the tightly coupled system is better than the loosely coupled system because individual pseudoranges can be accessed.

2.3. *Deeply Integrated System.* The terminology on the classification of integration architectures is not consistent. A good discussion on the use of this terminology is presented in Gautier (2003). Currently, there appears to be a number of ways of implementing deep integration or ultra-tight coupling (Gustafson et al., 2003; Gold et al., 2004). The main differences are in the implementation of the navigation filter. Examples here include the use of a minimum variance adaptive non-linear filter (Gustafson et al., 2003) and a standard Kalman filter (Kim et al., 2003). Apart from filter variations, there are various methods used to aid the GPS receiver tracking loop (the electronic/software loop used to lock onto satellite signals), including a) velocity information directly from the INS output, and b) an estimation of the line of sight vectors from the host vehicle to the satellites using INS position and satellite ephemeris data. Because the tracking loop is aided by external information this approach is referred to as deep or ultra-tight integration.

Another interesting recent approach involves the estimation of correlation delay for each channel of the GPS receiver using measurements from available satellites and INS (Gustafson et al., 2003). This estimation is carried out by an adaptive non-linear model, enhancing the efficiency of the tracking loop. Effectively, the INS is in the feedback loop. In another approach, the correlator signals (internal GPS receiver signals that correlate received signals with the receiver generated replicas) are used in a bank of Kalman filters along with INS measurements to aid the tracking loop (Kim et al., 2003).

Generally, deep integration is more dependent on the characteristics of INS errors than the other architectures. If the calibration of the INS parameters by GPS measurements is not accurate, the GPS tracking loop will not be able to get useful information from the INS. This increases the time it takes to lock on to the satellites. In severe cases it can lead to instability.

3. FAILURE MODES. To analyse the integrity of integrated systems, the threats to performance should be identified and modelled. The failure modes associated with GPS, INS and the integrated system, are presented below.

3.1. *GPS Failure Modes.* GPS is a complex system consisting of the space, control and user segments. Failures could occur at different levels from the control segment, through signal generation, transmission and processing within the receiver. As some of the operational GPS satellites were launched many years before the achievement of Full Operational Capability (FOC), their payloads have aged with time thereby increasing the likelihood of age-related failures. Table 1 provides a summary of GPS failure modes as captured from existing literature (Ochieng et al.,

Table 1. GPS failure modes.

Code	Cause	Characteristics	Impact and Remarks
G1	Clock jump	This is a clock misbehaviour that results in an abrupt change in the transmitted signal without any notification.	Can result in a range error of thousands of metres.
G2	Clock drift	This type of clock misbehaviour introduces a slow ramp type error in the transmitted signal. It is difficult to detect because its signature resembles the typical relative motion of a satellite and GPS receiver.	PRN 23 on 1 January 2004 experienced a clock drift error that grew gradually to a few kilometres (GPS support centre, 2005).
G3	Incorrect modelling of orbital parameters	Orbital models consisting of satellite orbits and clock parameters are constantly updated by a large Kalman estimator maintained at the Master Control Station in Colorado, USA. These are then uploaded to the satellites. Any error in these parameters results in incorrect navigation message. The error in the orbit parameters increases with the time lapse between two consecutive uploads and can be in the form of a slow ramp in the range measurements.	This type of error might be corrected at the next upload normally after eight hours provided the error is detected. Its effect on positioning accuracy depends on the receiver position and geometry of available satellites. It could result in a range error of up to 40 metres (Ochieng et al., 2003).
G4	Ionization of satellite payload silicon material	The performance of integrated circuits in the satellite payload degrades due to bombardment of heavy ion cosmic rays and energy from the sun. This can lead to errors in the navigation data or range. There are two types of this phenomenon *a*) Single Event Upset (SEU) caused by temporary change in the circuitry and *b*) continuous accumulation of the radiated material in the solid state substrates to make the integrated circuit (IC) inoperative (CommDesign, 1999)	The ionization of Integrated Circuits (ICs) results in reduced lifespan. ICs operating in outer space are radiation-hardened to minimize damage by radiation. However, this process is very expensive (Cellere, 2006). Depending on the slot which the satellite occupies, the exposure to radiation varies and hence its detrimental effect may range from instant failure to slow degradation of performance over time.
G5	Non-standard code (NSC)	Block IIR satellites are equipped with Time Keeping Systems (TKS) to generate a 10·23 *MHz* signal. Anomalies can occur in the voltage controlled oscillator of these systems that are shown to be correlated to solar eclipses (Wu, 1999). This results in the issuance of the Non-Standard Code (NSC). NSC is also generated when TKS loops are open and telemetry data are output by the Navigation Data Unit (NDU).	Generation of NSC acts as a warning to the GPS receiver. A proper GPS receiver design should remove the relevant satellite from the position solution as it is a meaningless measurement. Otherwise the code lock loop could become unstable.

Table 1. (*Cont*.)

Code	Cause	Characteristics	Impact and Remarks
G6	Eclipse related trajectory changes	When a GPS satellite comes out of an eclipse, its trajectory is perturbed due to the effect of changing solar radiation pressure.	This can cause range errors of up to 30 *m* (Ochieng et. al. 2003).
G7	Satellite attitude instability	This results in power fluctuation and changes in the nominal Signal-to-Noise Ratio (SNR).	This can result in either loss of lock or a significant signal acquisition/re-acquisition time.
G8	Excessive solar interference	This can produce ionospheric scintillations that make the nominal ionospheric modelling in the receiver meaningless.	Could introduce errors in excess of tens of metres. In severe cases, loss of lock may occur.
G9	Power fluctuations	The transmitted power fluctuations can make it difficult to lock on to a signal.	Could result in loss of lock.
G10	RF filter failures	Due to filter failure, side lobes may be corrupted. There can be sudden jumps or slow fluctuation in signal frequencies.	This makes it difficult for typical antennae to lock on to signals.
G11	Onboard multipath, onboard interferences and signal reflections	This is due to different transmitting antennae present on the satellite payload.	Due to the increase in the number of signals as a result of GPS modernization, this error might increase in future. This is usually addressed in two ways ● Multiple antennae on satellites are positioned in a manner to minimize this error. However, this is complicated by the constraint of maintaining all antenna directions towards the Earth. ● The multipath error is calibrated on the ground. After calibration as in the case of a typical satellite, attitude error in the range of 10 *sec* of arc can be present in the line of sight (Lopes et al., 2000).
G12	Inter-channel bias	These biases are present between different channels on the satellite transmitters due to the differences in the positions of transmitting antennas on the satellite. Furthermore, antenna phase centre error is different for different transmitters.	These errors will have more effect when position solutions are formed using multiple frequencies. Precise calibration on the ground for each channel is required to remove these types of biases. For a typical satellite the error between L1 and L2 antennae phase centres can be half a metre in range, for a Block IIA satellite (NOAA, 2000).
G13	De-synchronization between data modulation and code	This manifests as a constant bias for a particular satellite.	If there is a de-synchronization error of one bit between data and code modulation it can amount to a delay equivalent to a range error of 1·5 *sec*.

Table 1. (*Cont.*)

Code	Cause	Characteristics	Impact and Remarks
G14	Jamming/intentional interference	This is the generation of a powerful radio frequency in the vicinity of the receiver to either cause loss of lock (jamming) or degrade navigation accuracy (interference). Another way is spoofing which is the intended injection of spurious GPS like signal. A GPS receiver that locks onto such signals will not be able to get meaningful measurements.	Interference from amateur radio operators is a potential threat to GPS signal integrity. Availability of commercial jammers can prevent a GPS receiver from tracking signals.
G15	Unintentional interference	These occur when a GPS receiver is used in the vicinity of an installation that generates radio frequencies in the GPS frequency range.	Harmonic emissions from commercial high power transmitters, ultra wideband radar, television, VHF, mobile satellite services and personal electronic devices can interfere with the GPS signals. Depending on the magnitude and frequency of the transgressing signal, the effect may range from additional noise in signal to complete loss of lock.
G16	Ionospheric errors	The ionospheric layer extends from 50 *km* to 1000 *km* above the Earth. Nominal errors may be corrected by dual frequency signal usage or mathematical models. However, during high solar activity large errors in signals are introduced due to scintillations which cannot be correct by dual frequency signal usage or mathematical models.	In severe cases, loss of lock may occur. Range errors of up to 100 m can result in the case of a single frequency receiver. The Klobuchar model broadcast in the navigation message can compensate typically 50% of the ionospheric delay during the conditions of benign atmosphere. Better performance is achieved from relative positioning and dual frequency measurements.
G17	Tropospheric errors	The tropospheric layer extends from the surface of the Earth up to about 50 *km*. It consists of wet and dry parts. The GPS signal is delayed in this layer due to bending and refraction.	Range errors of up to 25 m can result but sudden changes/tropospheric storms can result in loss of lock. In normal conditions, the dry part of the tropospheric delay (90% of the total) can be compensated for by conventional models.
G18	Multipath	These errors are the result of the reception of the GPS signal by the receiver after reflection from surrounding surfaces.	This depends on the operational environment of the receiver and in extreme cases can result in loss of lock.

Table 1. (*Cont.*)

Code	Cause	Characteristics	Impact and Remarks
G19	Receiver problems	Receiver design and development should be according to the GPS receiver specification documentation. Departure from adhering to these instructions results in anomalous situations.	Warnings were issued by the US Coast Guard that certain receivers are not integrated properly with other equipment such as AIS (Automatic Identification System), radar, etc. (RIN, 2005). It might be possible that transmitted satellites are unhealthy but receivers still process their data. An example is carrier phase-only receivers failing to read the NSC (Baker et al., 1998). A receiver cannot lock onto NSC hence this will affect the acquisition time in the case of serial receivers and inappropriate utilization of channels in parallel receivers.
G20	Human related failures	GPS as part of cockpit equipment results in overconfidence of the aircrew.	In July 2004, two accidents were reported ● Incorrect reliance on GPS killed 44 (RIN, 2005) ● Fatal GPS Approach (RIN, 2005)
G21	Low Availability	The number of available satellites may not always be sufficient to provide good geometry in all areas of the Earth.	Examples include: ● Poor geometry available over the UK in May 2004 (RIN, 2005). ● The Great Lakes area in the United States was reported to have experienced poor geometry. (Ocean Teacher, 2006).
G22	Single-String Failure Mode	One or both of two critical subsystems – the satellite bus and the navigation payload are operating without backup capacity.	At any time, 16 satellites may be operating in single string failure mode (Gibbons, 2002). The non-availability of backup results in the shutting down of the satellite signal in case of failure of the primary critical sub-system.
G23	Leap Second Anomaly	This primarily results in a timing error that degrades navigation accuracy.	On 28th November 2003, a leap second anomaly was experienced by many GPS receivers (GPS support centre, 2005). Receivers might lose track for a second before recovering.

2003), augmented with new ones identified in this paper. Each failure mode is assigned a unique identification (ID), with a corresponding summary which includes an estimate of its impact on the relevant measurements. The ID is used later in the paper to facilitate grouping of failure modes so that models can be specified for each group.

3.2. *Inertial Navigation System Failure Modes.* An INS consists of a sensor arrangement (gyroscopes and accelerometers) and a navigation processor. The measurements obtained from the gyroscopes and accelerometers i.e. angular rates and accelerations are integrated in a navigation processor to obtain the position solution. Any hardware errors or errors in initial conditions act as forcing functions to the navigation mechanization equations and hence grow with time. Hence, over time, these nominal errors convert into failures depending on the requirements set for particular applications. In aviation, for example, nominal INS errors become failures when the alert limits set by ICAO are exceeded. This section describes three classes of INS failure modes: those arising from operational hardware, operational software and those specific to MEMS technology.

3.2.1. *INS Operational Hardware Failure Modes.* INS operational hardware failure modes are in fact nominal hardware INS errors that are well known in the navigation community. Table 2 presents these failures. They have been compiled from existing research literature (Farell, 1976; Titterton et al., 1997; Farell et al., 1998; Madni et al., 2001; White et al., 2002).

3.2.2. *INS Operational Software Failure Modes.* INS software failure modes (presented in Table 3) are associated with the navigation software mechanization. The navigation equations are driven by the initial conditions and outputs from the sensors. Hence, errors in the initial conditions and outputs of sensors grow with time due to the integration of navigation equations in the navigation processor. In order to study their effects, error models with temporal growth characteristics are typically used. It is not possible to use these models for on-line compensation because of the random nature of their initial conditions and errors of sensors. For example, although it is known that Schuler oscillation has a time period of around 84 minutes and its behaviour is sinusoidal, the sign and the magnitude varies with the quality of the initial conditions and sensors used (Farrell, 1976; Titterton et al., 1997).

3.2.3. *MEMS-based INS Failure Modes.* MEMS technology based sensors are etched from silicon wafer based on Integrated Circuit (IC) fabrication technology. In contrast to typical IC electronic circuits, a MEMS-based INS contains moving elements. Hence, there are frictional errors associated with the movement of surfaces. It should be noted that research on MEMS-based failures in the literature is mostly limited to assessment of reliability in harsh environments. There is limited research on gradual performance degradation which is more relevant to INS sensors. The potential MEMS-based INS material failure modes are present in Table 4.

3.3. *Integrated System Failure Modes.* When two systems are integrated, failure modes can result from the integration process. The failure modes (listed in Table 5) arise from the formulation of the integration filter and the interaction of two systems. It should be noted that due to the complex nature of the coupling between two systems, it is not always possible to quantify the impact of these failure modes.

Table 2. INS hardware failure modes.

Code	Cause	Characteristics	Impact and Remarks
IO1	Poor calibration	The calibration of INS sensors is done in sophisticated laboratories. Calibration of gyroscopes is done by precision rate tables and that of accelerometers by precision dividing head tables (Titterton et al., 1997). This results in precise calibration constants that are applied to measurements obtained from sensors. The calibration constants may be wrong due to human error, calibration time expiry, errors in the calibration laboratory setup *etc*. This will lead to inaccurate values supplied to the navigation processor in an INS.	The calibration of INS is an expensive process carried out periodically. The period of calibration depends upon the quality of the INS used, as ageing affects the quality of calibration parameters. In the case of the gyro torquer calibration (in the mechanical gyroscope) an error 0·1% can lead to a drift rate of 0·01 *deg/hr* at speed of 600 *knots* (Farrell, 1976).
IO2	Random gyroscope drift	This is due to the random nature of the error that is present in the output of inertial sensors.	This is the most common gyroscope error and has the worst effect on the performance of the navigation system. For this reason, gyroscopes are classified on the basis of random drift. An inertial grade gyroscope having a drift error specification of 0·01 *deg/hr* can introduce an error of 1 *nmi/hr* in the position solution.
IO3	Random walk	The integration of a random variable results in a random walk process. It is due to the construction process of fibre optic based, ring laser or MEMS based gyroscopes.	When this error is present (does not exist in conventional mechanical gyroscopes) it is the second most important specified error. For an inertial grade gyroscope a position error around 1 *nmi/hr* can result from a random walk error of 0·001 $deg/\sqrt{hr}$.
IO4	Random noise	This type of noise is present in the inherent physical process of measurement. It could also be due to the nature of the front end signal processing.	Usage of signal filters with limited bandwidth can reduce this error below the minimum nominal measurement signal. A typical MEMS technology gyroscope can have noise error equal to 0·5 *deg/sec rms* (BAE systems, 2006).
IO5	Non-linearity	The physical measurement processes are non-linear but linear models are used to describe them.	Detailed calibration models can be used to reduce non-linearity effects. A typical MEMS technology based accelerometer can have a non-linearity error of up to 2000 *ppm* (1 sigma) (BAE systems, 2006).
IO6	Out of range	This failure mode can arise when the INS sensor reaches its operational limit.	Mechanical stops are designed to reduce damage to the sensor in case of out of range operation. The INS will be unable to measure any parameter out of range. The magnitude of error will depend on the applied angular rate and the operating range of the sensor.

Table 2. (*Cont*.)

Code	Cause	Characteristics	Impact and Remarks
IO7	Alignment error	The INS platform should be aligned to the measurement axis. An offset between the two axes is referred to as an alignment error.	Precise casings are used for minimizing this error. Similarly, initial starting position values need to be determined precisely. For a typical MEMS technology INS, axis alignment may be around 400 *micro-rad* (BAE systems, 2006). This error can translate to about 15 *m* in horizontal position error in a level flight in 1 *min*.
IO8	Scale factor stability	The relation between the output and input of the sensor is the scale factor.	The scale factor of the INS measurement is estimated through the calibration process. An error in the estimation will result in degraded performance. The typical error in the calibrated and the true scale factor is in the range of 0·1–2% (Titterton, 1997).
IO9	G-squared sensitivity	Gyroscopes are also sensitive to acceleration and its squared value.	A typical fibre-optic gyroscope can have a g-dependent bias around 1 $deg/hr/g$ and g^2 dependent bias around 0·1 $deg/hr/g^2$.
IO10	Electromagnetic Interference (EMI)	Although INS are typically immune to external interference, strong EMI near an airport may have an adverse effect on the performance of the INS.	INS memory scrambling has been reported in the vicinity of strong radio transmitters (Shooman, 1994).
IO11	Bias	Bias is any offset present in the measurement of a gyroscope or an accelerometer; a result of mechanical imperfection.	A fixed bias can be estimated during the process of calibration. Bias stability refers to the stability of this value during the operation of the sensor. It is the most important error in the operation of an accelerometer. Typically an inertial grade accelerometer has a bias error value of 10 *micro-g* (1 sigma).
IO12	Sign asymmetry	It is possible that when a gyroscope or accelerometer measures negative or positive quantities there is a difference in the scale factor in both directions.	This can be a source of error when the calibration setup is not available in both directions due to calibration equipment limitations. In that case the difference in two axes will remain introducing an equivalent error in the output.
IO13	Dead zone	This is a zone surrounding the zero measurement where there is no response at the output even if the input varies.	This limits the operation of sensors at low values within the zone. This is a typical characteristic of Ring Laser Gyroscopes referred to as the lock-in problem. In this problem the observable frequency difference is zero at a certain input. Using very high quality mirrors it can be brought down to less than the rate of rotation of the earth (15 deg/hr). Sophisticated techniques based on artificial biasing are used to reduce it further (Faucheux et al., 1988).

Table 2. (*Cont.*)

Code	Cause	Characteristics	Impact and Remarks
IO14	Quantization error	This is due to the conversion of analogue measurements into digital form.	If in an INS, the output of the gyroscope is sampled at 100 *Hz*, for an input of 10 *deg/s* there can be an error of 0·1 *deg/s* due to quantization. This error is not present in gyroscopic devices whose observable is frequency difference where there is no need for an analogue to digital converter. An example is the fibre-optic based gyroscope.
IO15	Anisoinertia errors	This type of error arises typically in the spinning mass gyroscope and is due to inequalities in a gyroscope's moments of inertia about different axes. The resulting bias is proportional to the product of angular rates applied about pairs of orthogonal axes.	For modern Dynamically Tuned Gyroscopes (DTG) designed for maximum continuous rate of 900 *deg/sec*, the error due to anisoinertia can be 100 *deg/hour* (Lee et al., 1997).
IO16	Sensitivity/ Resolution	This is a measure of the ability of a sensor to detect small changes in a variable that is to be measured.	This can be a source of error, if the angular rate or acceleration value is not within the sensitivity of the sensor. It can be due to the limitation of the sensor itself or the signal processing circuitry. In the case of a typical strapdown sensor that operates over a wide range *e.g*. from less than 0·1 *deg/sec* to 100 *deg/sec*, a single calibration coefficient set cannot be justified for the whole range. Hence, error is introduced especially at higher values of the applied input rate.
IO17	Vibration modes	Errors arise from the impact of vibration on gyroscope and accelerometer measurement processes.	The base of INS is designed to minimize the impact of vibration and if possible to install INS away from the vibration source. An example of extreme vibration is presented by Ledroz (2005) for FOG (although containing no moving parts) for which a drift in the azimuth of about 2 *deg* per 5 *min* is reported.
IO18	General errors	Other potential error sources include: a) Power failure b) Lightning c) Fungus d) Voltage spike e) Operational shock	 Battery power may not last for the whole operation of flight. A stroke of lightning may disrupt the operation of INS completely. The required humidity level should be maintained to prevent accumulation of fungus in or around INS sensors. Voltage spikes can result in the electronic circuitry and can disrupt the operation of the sensor. In INS sensor specifications, the worst case shock limits are listed. Any values beyond these can result in a physical breakdown of a device.

Table 3. INS software failure modes.

Code	Cause	Characteristics	Impact and Remarks
IOS1	Schuler oscillation error	This is sinusoidal in nature and is due to the combination of initialisation errors and the inherent nature of navigation mechanization equations.	This type of error propagates over a long period of time and has a time period of about 84 *min*. A large and increasing error can result by stimulation of the Schuler loop. For example, an aircraft executing a series of 180 *deg* turns at an interval of 42 *min* can produce this type of error (Titterton et al., 1997).
IOS2	Gravity model errors	In the navigation mechanization, the gravity model must be incorporated as accelerometers are unable to differentiate between gravity and applied acceleration.	Gravity models are complex. Hence, truncated models are usually used. For typical aviation applications models accurate to 1 *milli g* are required.
IOS3	Coning	This error is due to the motion which arises when a single axis of a body describes a cone.	The coning correction is important for specific trajectories of the host vehicle. Hence, an assessment of this error for the trajectory should be carried out. Coning motion of 0·1 *deg* at a frequency of 50 *Hz* can result in the computed attitude error of 100 *deg/hr* (Titterton et al., 1997).
IOS4	Sculling	This type of error is due to the combination of linear and angular oscillatory motions of a host vehicle that are of equal frequency in orthogonal axes.	As for the coning correction this is also important when specific manoeuvres arise during the course of the trajectory. Such a situation might arise when an aircraft experiences a tight turn. For an acceleration of 10 *g* and a vehicle rotation of 0·1 *deg*, an acceleration bias equivalent to 9 *milli g* can result (Titterton et al., 1997).
IOS5	Altitude instability	The vertical channel of INS is unstable and hence barometers may be used to stabilize this channel.	This in turn introduces new issues that need to be resolved, such as the order and stability of the barometer loop. The vertical channel instability of un-aided IMU results in increasing error in height so that this value becomes useless in a matter of minutes of flight.
IOS6	Model of the Earth	Depending on the accuracy required, the Earth model is assumed to be flat, spherical or ellipsoidal each with its accuracy limitations.	For long haul flights an ellipsoidal model of Earth is to be used. At the poles a spherical earth model can produce an error of 20 *km* as compared to the ellipsoidal model.
IOS7	Initialization errors	A potential source of error is due to incorrect initial conditions. These conditions are required for the solution of differential equations.	High accuracy is to be maintained in this aspect. This is achieved by the use of pre-determined high accuracy positioning data. For example if we assume there is only a velocity error of 0·1 *m/s* in the initial condition, it can create a horizontal position error of 30 *m* in 5 *min* in typical conditions.
IOS8	Foucault and 24 *hr* oscillations	Foucault oscillation is a long-period oscillation which maintains itself as a modulation of the Schuler oscillation while 24 *hr* oscillation present in the INS solution is related to the period of the rotation of the Earth.	The period of Foucault oscillation is about 30 *hr* for moderate latitudes. These are included here for the sake of completeness as the magnitude of errors induced by them for a nominal flight is in the order of centimetres.
IOS9	Integration method	As INS propagation equations are analogue in nature, the accuracy is limited by the choice of the integration method.	In the past, two speed algorithms have been utilized because of computation limitations. Slowly moving variables are computed at a slow rate while a high computation rate is used for fast moving variables. However, using fast computers of today, sophisticated algorithms are designed to remove the error induced by the integration method. For a typical aircraft INS an error rate of 0·00037 *deg/hr* is estimated for coning algorithm (Savage, 1999).

Table 4. MEMS-based INS material failure modes.

Code	Cause	Characteristics	Impact and Remarks
IM1	Fracture	Any process that results in an irreversible repositioning of atoms within a material can contribute to fatigue and hence result in fracture (Brown et al., 1996).	Periodic Built in Tests (BIT) may be useful in the detection of this type of failure mode. The sensor will cease to work in this case.
IM2	Creep	This is a time-dependent mass transfer through glide and diffusion mechanisms in materials due to high stresses or stress gradients (Brown et al., 1996) or due to the slow movement of atoms under mechanical stress.	This slow failure mode can degrade the inertial sensing of the sensor as part of the ageing process.
IM3	Stiction	This is the effect of sticking together of surfaces in MEMS structures due to surface forces. The most important surface forces are the capillary force, the molecular Van der Waals force and the electrostatic force.	These forces dominate due to the small sizes of MEMS based sensors (Spengen, 2003). The sensor with the sticked sensing element may produce erroneous maximum value.
IM4	Friction and wear	Adhesive wear is more important in MEMS in which contact surfaces partly adhere to each other at their highest points (Spengen, 2003).	Built in Tests might be useful in this regard. The effect will be progressive degradation of sensor accuracy.
IM5	Dielectric charging and breakdown	There is potential for building-up of charges in MEMS sensors with dielectric layers.	Sensors are known to drift over time due to the charge accumulation on the surface.
IM6	Contamination	Contamination of the sensor can be due to humid environments in which the sensor is placed.	This will degrade the performance of the sensing element. Suitable hermetic packaging is to be designed to avoid contamination.
IM7	Electro-migration	This is due to forced atomic diffusion with the driving force due to an electric field and associated electric currents in a metal. (Pierce et al., 1997).	This is an important failure mode in the metallization of integrated circuits. Proper shielding may prevent this error.
IM8	Delamination	High stresses can be associated with multi-layer films introduced by processing, thermal mismatch or epitaxial mismatch.	The adhesion between layers depends strongly on their chemical and mechanical compatibility (Brown et al., 1996). This failure mode is relevant for pendulous accelerometers.
IM9	Pitting	Formation of small craters or pits on the surface of metals.	Pitting and hardening can be decreased by reducing the actuation force. It affects the balanced loop output of resonant structures in gyroscopes which is crucial in angular rate measurements (Sparks et al., 2001). The consideration of pitting during the design process can limit its available range of measurement.
IM10	Radiation damage	Radiation may damage the sensitive sensing element of the sensor.	A comparison of two accelerometers with respect to the response to irradiation shows that accelerometers in which dielectric layers are covered with a conducting layer suffer very little change in the output voltage in contrast to accelerometers having no such layer (Knudson et al., 1996).
IM11	Thermal effects	Mismatched thermal expansion coefficients can also cause interface failure.	Reliability can be improved taking into account such considerations. From an operational point of view, thermal cycling stability is important and is to be ensured for stable performance (Madni et al., 2001). However, as shown in Ghaffarian et al. (2002) and Sharma et al. (2000), EMS accelerometers are capable of sustaining a range of thermal and mechanical reliability tests.

Table 5. Integrated system failure modes.

Code	Cause	Characteristics	Impact and Remarks
INT1	Erroneous in-flight calibration	The calibration may be erroneous as a result of erroneous GPS measurements, causing the errors to propagate.	Low cost sensors are required to be calibrated more frequently to minimize errors. Calibration also needs a finite amount of time for convergence (Groves et al., 2002). This error affects the ultra tightly coupled architecture the most because of the presence of feedback loop between the two component systems.
INT2	Divergence of Kalman filter	If there is a rapid change in filter gains, Kalman filters may diverge so that the output becomes unstable (Jwo et al., 1996).	Filter integrity management that involves pre-checks of measurements before the update step can help in removing this failure mode. In a loosely coupled system, the chance of divergence of the Kalman filter is low but these are more probable in the tightly coupled and the ultra tightly coupled systems.
INT3	Tracking loss due to erroneous INS output	The type of integration architecture depends on the reliance of GPS on the INS output. When the GPS tracking loop is increasingly dependent on the INS output, it may create loss of lock in case of erroneous INS output (Jwo et al., 1996; Gautier, 2003).	This error will be dominant in less accurate inertial navigation systems such as those based on MEMS technology and ultra tightly coupled systems.
INT4	Tracking loop noise bandwidth	The stability of the tracking loop depends on the magnitude of the noise bandwidth. Instability can result if it is too small or too large (Jwo et al., 1996).	If the bandwidth is wide, less noise will be filtered out but if it is small, then the performance of the tracking loop will be degraded. Hence, a trade-off should be made during design. This error is specific to the ultra tightly coupled system.
INT5	Observability of INS parameters	Due to the frequent calibration requirement of INS, the parameters of INS must be observable. However, this is not always the case and specific manoeuvres are required for the calibration of certain parameters (Hwang et al., 2000; Hong et al., 2002, 2005; Chiang, 2003; Eck et al., 2003).	Another possibility is the usage of multiple GPS antennas for calibration of INS parameters (Wagner, 2005). This situation mostly affects ultra tightly coupled systems because of the dependence of the GPS receiver processor on the operation of INS.
INT6	Incomplete modelling and initial conditions	Real life processes are non-linear while typical use of the Kalman filter is linear. Hence, there are model uncertainties which can cause errors. Similarly, the tuning parameters of the Kalman filter that include variances for the process and sensor noise often rely on experience (He et al., 1999; Bruner, 2000; Klotz et al., 2000; Chiang 2003). Incorrect parameters lead to instability.	An example is presented in Rogers (2001) on the assumption of small azimuth errors and its validity in operational situations. The usage of the Kalman filter requires an update of the linearized system matrix at a suitable sampling interval (rate). There are many approximate methods for the update of such a linearized system matrix (Moler et al. 2003). All of these methods work on assumptions regarding the elements of the matrix to be updated. A wrong choice of method may lead to instability. This error affects all types of integration architectures.

Table 5. (*Cont.*)

Code	Cause	Characteristics	Impact and Remarks
INT7	GPS measurement delay	An INS outputs data at a rate faster than GPS e.g. typically at 20 *ms*. Low cost GPS receivers have a data update rate of 1 *sec*, hence creating an anomaly.	Two methods to tackle this anomaly are presented in Eck et al. (2003). One is based on the extrapolation of GPS measurements and the other on the computed measurement error due to previous GPS measurements. This error affects all types of integration architectures.
INT8	Transients at the satellite changeover	The Kalman filter estimates the clock biases and drifts for satellites that are included in measurements. However, when there is a changeover in participating satellites, the filter has to renew the estimation of the biases. This introduces transients and is a source of error (Moore et al., 1995; Groves et al., 2002).	Special algorithms are used that take care of satellite changeovers by changing the appropriate rows and columns of the Kalman filter. This type of error affects tightly coupled and ultra-tightly coupled systems. Loosely coupled systems are affected in the case when it is not possible for a receiver to compute the antenna position due to the lack of available satellite measurements.
INT9	Gaussian assumption	A Kalman filter works on the assumption that the sensor noise and processor noise are Gaussian and unbiased.	This assumption does not hold in practice always and may result in a degraded position solution. This error affects the system in which Kalman filtering is used. It is not applicable in the case of couplings where a non-linear processor is used (Gustafson et al., 2003).
INT10	Lever arm correction	An important correction is the physical location of the GPS receiver and INS on the instrument panel. Long lever arm distances are suggested for better accuracy of the attitude output (Wagner et al., 2002).	Similarly, flexure in the lever arm is to be accounted for (Cox, 1998; Wagner et al., 2005). If not properly accounted for, this affects all types of integration architectures.
INT11	Correlation	The Kalman filter formulation is based on the assumption that measurements are independent.	Due to the integration of sensor measurements, this may not always be the case. Hence, modelling errors may be introduced. This error affects the system in which Kalman filtering is used. It is not applicable in the case of couplings where a non-linear processor is used (Gustafson et al., 2003).

Table 6. Failure mode characterization, groups and models.

Error Type	Related Codes	Failure Model	Remarks
Step Error	G1, G5, G6, G9, G10, G14, G20, G22, IO18(a), 1O18(b), IO18(d), IO18(e), IM1, IM3, IM5, IM8, INT2, INT3, INT4, INT8	$f(t) = A\ u(t - t_0)$ Where A is the magnitude of the fault, $u(t)$ is the unit step function and t_0 is the onset time of the failure.	These errors can easily be detected by Snapshot integrity methods. These methods are based on current measurements as opposed to averaging methods and are less computationally intensive. The failure model that is proposed here covers the class of sudden failures with magnitudes larger than a given threshold.
Ramp Error/ Drift	G2, G3, G21, IO1, IO2, IO7, IO9, IO14, IOS5, IOS7, IOS9, IM5, IM9, INT1, INT5, INT6	$f(t) = R(t - t_0)\ u(t - t_0)$ Where R is the slope of the fault, $u(t)$ is the unit step function and t_0 is the onset time of the failure	This type of error is the most difficult to detect early when the slope is small. Snapshot methods can detect these faults only when the accumulated error goes beyond a pre-determined threshold. Ageing of equipment can contribute to these types of failures.
Random Noise	G3, G4, G7, G8, G11, G12, G15, G16, G17, G18, G19, IO1, IO4, IO5, IO6, IO8, IO10, IO12, IO15, IO17, IO18(c), IOS6, IM2, IM4, IM6, IM7, IM10, IM11, INT9	$f(t) = A_k\ u(t - t_0)$ where $A_k \sim \begin{cases} N(0, \Sigma_k) & k < t_0 \\ N(\eta(k, t_o), \Sigma_k) & k \geqslant t_o \end{cases}$ where $N(m,V)$ describes Gaussian normal distribution with mean m, η is the mean value of the fault and variance V, u(t) is the unit step function and t_0 is the onset time of the failure.	This category covers many types of errors, from ionospheric scintillation and tropospheric variations to various processes in the INS.

Table 6. (*Cont.*)

Error Type	Related Codes	Failure Model	Remarks
Random Walk	IO3	$$\dot{f}(t) = a(t)/\sqrt{dt}\ u(t-t_0)$$ $a(t)$ is a random variable with gaussian statistical distribution as defined in the above row, $u(t)$ is the unit step function and t_0 is the onset time of the failure.	This failure mode is significant in fibre-optic based, ring laser and MEMS technology based gyroscopes. It is also present in MEMS technology based accelerometers.
Oscillation	IOS1, IOS2, IOS3, IOS4, IOS7, IOS8	$$f(t) = A\ \sin(t-\theta)\ u(t-t_0)$$ A is the magnitude of the fault, θ is the phase difference, $u(t)$ is the unit step function and t_0 is the onset time of the failure.	In navigation equation mechanizations, oscillatory behaviour results from the modelling of the Earth's dynamics, feedback effect of initial conditions and calibration errors.
Bias	G6, G13, G19, IO11, IO13, IO16, INT7, INT10, INT11, G23	$$f(t) = B\ u(t-t_0)$$ Where B is the magnitude of the fault, $u(t)$ is the unit step function and t_0 is the onset time of the failure.	Bias can be considered as a small constant error which is less than the pre-determined error threshold of the integrity algorithm. Hence this cannot be detected. This type of error is significant in the case of occurrence of simultaneous multiple failure modes. In that case it is possible that two or more faults each having an error less than the threshold may create an effect in the position solution that is more than that due to error threshold (Hwang et al., 2005). Ageing of equipment can also contribute to this type of failure.

4. CLASSIFICATION OF ERRORS. Before assessing the capability of integrity algorithms to protect against the failures above, mathematical models for failures are required. Such models enable integrity performance to be studied by simulation. The first step in the failure modelling process is to group failure modes into classes which enable mathematical functions (representing each class) to be developed (Table 6). Intuitively, the class of errors that has the largest number of entries is random noise.

With respect to the characterization in Table 6, two points are to be noted here:

- The models shown do not represent the properties of the failure modes exactly. Rather, they are assigned on the basis of their approximate growth and magnitude characteristics, as these have the most relevance for integrity algorithms.
- There are codes which are present in more than one classification, the reason being that some errors like IOS7 are oscillatory in nature but their magnitude also drifts with time.

5. CONCLUSION. This paper has presented the failure modes and models of the integrated GPS/INS architectures. The failure models, although not rigorous are potentially useful in a simulation environment to facilitate the specification of effective integrity monitoring methods and algorithms.

ACKNOWLEDGEMENTS

The authors acknowledge the financial support from the Government of Pakistan, Imperial College London and Dr. Imran Iqbal Bhatti.

REFERENCES

Babu, RW. (2004). Improving the Quality of IMU-Derived Doppler Estimates for Ultra-Tight GPS/INS Integration. In: Proceedings of the ENC, Rotterdam, Netherlands, paper 144, pp 1–8.

BAE Systems (2006). Inertial products data sheets. http://www.baesystems-ps.com/

Baker, BC., Huser, SJ (1998). Protect Yourself! Navigation Payload Anomalies and the Importance of Adhering to ICD-GPS-200. In: Proceedings of the Technical Meeting of the Satellite Division of the Institute of Navigation, Tennessee, USA.

Brown, SB., Jansen, E (1996). Reliability and Long Term Stability of MEMS. In: Advanced Applications of Lasers in Materials Processing, IEEE, Colorado, USA.

Bruner, CP (2000). LN-200G first SAASM based tactical grade INS/GPS Navigator. In: Proceedings of the Technical meeting of the Satellite Division of the Institute of, Salt Lake city, Utah, USA.

Chiang, K-W (2003). The utilization of single point positioning and a multi-layers feed-forward network for INS/GPS Integration. In: Proceedings of the Technical meeting of the Satellite Division of the Institute of Navigation, Portland, Oregon, USA.

Cellere, G (2006). Personal Comm. Dept of Information Engineering, University of Padova, Italy.

CommDesign (1999). http://www.commsdesign.com/main/1999/11/9911feat2.htm

Cox, DB (1998). Integration of GPS with Inertial Navigation Systems. Global Positioning Systems and its Augmentations, I:pages 144–153.

Eck, C., Kottmann, M., Geering, HP (2003). Analysis of GPS measurement delays in low-cost INS/GPS navigation systems. In: ION GPS/GNSS 2003, Portland, Oregon, USA.

Farrell, JL (1976). Integrated Aircraft Navigation. Academic Press Inc., San Diego, California.

Farrell, JL., Barth, M (1998). The GPS and Inertial Navigation. Mc-Graw-Hill, New York.

https://doi.org/10.1017/S0373463307004237 Published online by Cambridge University Press

Faucheux, M., Fayoux, D., Roland JJ (1988). The Ring Laser Gyro, J. Otpics, 19(3):pages 101–115.

Gautier J (2003) GPS/INS generalized evaluation tool for the design and testing of integrated navigation systems. PhD Thesis, Stanford University, USA.

Ghaffarian, RJ., Sutton, DG., Chafee, P., Marquez, N., Sharma, A., Teverovsky, A (2002). Thermal and Mechanical Reliability of Five LOTS MEMS Accelerometers. White paper. NASA Electronics Parts and Packaging Program, USA.

Gibbons, G (2002). Is the Sky Falling? GPS World.

Gold, KL., Brown, AK (2004). A Hybrid Integrity solution for Precision Landing and Guidance. In: Proceedings of IEEE PLANS, IEEE, California, USA, pp 165–174.

GPS Support Centre website http://www.schriever.af.mil/GpsSupportCenter/

Groves, PD., Wilson, GG., Mather, CJ (2002). Robust rapid transfer alignment with an INS/GPS reference. In: Proceedings of the National Technical Meeting, ION, San Diego, pp 301–311.

Gustafson, D., Dowdle, J (2003). Deeply integrated code tracking: comparative performance analysis. In: Proceedings of ION GPS/GNSS 2003, Portland, Oregon, pp 2553–2561.

He, XF., Vk, B (1999). Use of extended interval Kalman filter on integtrated GPS/INS system. In: Proceedings of the Technical meeting of the Satellite Division of the Institute of Navigation, Nashville.

Hong, S., Zhang, YS., Ha, S-K., Lee, M-H (2002). Estimation of Alignment errors in GPS/INS integration. In: Proceedings of the ION GPS 2002, Portland, Oregan, USA.

Hong, S., Lee, MH., Chun, H-H., Kwon, S-H., Speyer, JL (2005). Observability of Error States in GPS/INS Integration. IEEE Transactions on Vehicular Technology, 54(2), 731–743.

ICAO (2004). Annex 10: International Standards and Recommended Practices. Aeronautical Telecommunications, Volume 1.

Hwang, D-H., Kim, YS., Oh, SH., Lee, SJ (2000). Performance Improvement of the Attitude GPS Aided SDINS Alignment. In: Proceedings of the 13th International Technical meeting of the Satellite Division of the Institute of Navigation, Salt Lake City, Utah, USA.

Hwang, PY., Brown, RG (2005). NIORAIM Integrity Monitoring Performance In Simultaneous Two-Fault Satellite Scenarios. In: ION GNSS 2005, Institute of Navigation, San Diego, California, USA.

Jwo, D-J., Tuckness DG (1996). On the Stability Investigation of Integrated GPS/INS navigation systems. In: Proceedings of the 9th International Technical meeting of the Satellite Division of the Institute of Navigation, Kansas City, Missouri, USA.

Kim, H-S., Bu, S-C., Jee, G-I., Gook, C., Park (2003). An ultra-tightly coupled GPS/INS integration using federated Kalman filter. In: Proceedings of ION GPS/GNSS 2003, Portland, Oregon, USA.

Klotz, HA., Reynolds, AHI (2000). Evaluating Anti-Jam GPS/INS System Performance. In: Proceedings of the National Technical Meeting, Institute of Navigation, Anaheim, California, USA.

Knudson, AR., Buchner, S., McDonald, P., Stapor, WJ., Campbell, AB., Rabowski, KS., Knies, DL (1996). The Effects of Radiation on MEMS Accelerometers. IEEE Transactions on Nuclear Science, 43(6):pages 3122–3126.

Lee, YC., Ericson, SD (2004). Analysis of Coast Times Upon Loss of GPS Signals for Integrated GPS/Inertial Systems. Air Traffic Control Quarterly, 12(1), 27–51.

Lee, S-K., Lee, C-W (1997). Errors of the dynamically tuned strapdown gyroscope to constant and harmonic rate inputs. In: Proceedings of Institute of Mechanical Engineers, 21(C):pages 627–637.

Ledroz, AG., Pecht, E., Cramer, D., Mintchev, MP (2005). FOG-Based Navigation in Downhold Environment During Horizontal Drilling Utilizing a Complete Inertial Measurement Unit: Directional Measurement-While-Drilling Surveying. IEEE Transactions on Instrumentation and Measurement, 54(5):pages 1997–2006.

Lopes, RVF., Milani, PG (2000). Consistent On-board Multipath calibration for GPS based spacecraft Attitude Determination. In: Proceedings of the 13th International Technical meeting, Institute of Navigation, Salt Lake city, Utah, USA.

Madni, AM., Costlow, LE (2001). A third generation, Highly Monitored, Micromachined Quartz Rate Sensor for Safety-Critical vehicle stability control. In: IEEE Proceedings, Montana, USA.

Moler, C., Loan, CV (2003). Nineteen Dubious Ways to Compute the Exponential of a Matrix, Twenty Five Years Later. SIAM REVIEW, 45(1):pages 3–49.

Moore, T., Rudolph, K., Ziolkowski, F., Luckau, A (1995). Use of the GPS Aided Inertial Navigation System in the Navy Standard Missile for the BMDO/Navy LEAP Technology Demonstration Program. In: Proceedings of the 8th International Technical Meeting, Institute of Navigation, Palm Springs, USA.

NOAA website (2006). http://www.ngs.noaa.gov/ANTCAL/Satellites/Blk2a/

Ocean Teacher (2006). http://ioc.unesco.org/oceanteacher

Pierce, D., Brusius, P (1997). Electromigration: A review. Microelectronics Reliability, 37(7):1053–1072.

Ochieng, WY., Sauer, K., Walsh, D., Brodin, G., Griffin, S., Denney, M (2003). GPS integrity and potential impact on aviation safety. Journal of Navigation, 56(1), 51–65.

Rogers, RM (2001). Large Azimuth INS Error Models for In-Motion Alignment. In: Proceedings of the National Technical Meeting, Institute of Navigation, Long Beach, California, USA.

Royal Institute of Navigation (2005). GPS news archives. www.rin.org.uk.

Savage, PG (1999). Strapdown Inertial Navigation Integration Algorithm Design Part 1: Attitude Algorithms. Journal of Guidance, control and dynamics, 21(1).

Sharma, AK., Teverovsky, A (2000). Evaluation of Thermo-Mechanical Stability of COTS Dual-Axis MEMS Accelerometers for Space Applications. In: Proceedings of COTS MEMS conference, Knowledge Foundation, Berkley, California, USA.

Shooman, ML (1994). A study of occurrence rate of Electromagnetic Interference (EMI) to Aircraft without a focus on HIRF (External) High Intensity Radiation Fields. NASA CR 194895

Sparks, D., Chia, M., Zarabadi, S (2001). Reliability of Resonant Micromachined Sensors and Actuators. In: SAE World congress, Society of Automotive Engineers, International, Detroit, USA.

Spengen, WMV (2003). MEMS reliability from a failure mechanisms perspective. Microelectronics Reliability, 43(7):pages 1049–1060.

Titterton, DH., Weston, JL (1997). Strapdown Inertial navigation technology. Peter Peregrinus Press.

US DoD (2001). GPS Standard Positioning Service Performance Standard.

Van Dyke K, Kovach K, Lavrakas J, Carroll B (2004) Status Update on GPS Integrity Failure Modes and Effect Analysis. In: Proceedings of ION 2004 National Technical Meeting, San Diego, USA.

Volpe Report (2001). Vulnerability Assessment of the Transportation Infrastructure relying on the Global Positioning System. John A. Volpe National Transportation Policy, August 29.

Wagner, JG., Kasties, G (2002). Improving the GPS/INS integrated system performance by increasing the distance between GPS antennas and inertial sensors. In: Proceedings of the National Technical Meeting " Integrating Technology", San Diego, California, USA.

Wagner, JF (2005). GNSS/INS integration: still an attractive candidate for automatic landing systems? GPS solutions, 9(3):pages 179–193.

White, E., Rios, JA (2002). FAA certification of a MEMS attitude and Heading Reference system. In: Proceedings of the National Technical Meeting, ION, San Diego.

Wu, A (1999). Investigation of the GPS Block IIR Time Keeping System (TKS) anomalies caused by the voltage-controlled crystal oscillator. In: 31st Annual PTTI Meeting, California, USA.

Wagner, JF., Wieneke, T (2003). Integrating satellite and inertial navigation – conventional and new fusion approaches. Control Engineering Practice, 11, 543–550.